CMOS Neural Probe With Multi-Turn Micro-coil Magnetic Stimulation

Edward C. Szoka[1], Jesse C. Werth[2], Thomas A. Cleland[2], Shelley Fried[3], Alyosha Molnar[1]

***Abstract*— Micro-coil magnetic stimulation has been shown to be an effective method of neurostimulation while circumventing issues that limit the more commonly used implantable electrodes. Micro-coils do not need direct electrical contact with biological tissue, allowing for complete device encapsulation. This allows for the stimulation effectiveness to be maintained over long periods of time and eliminates the electrode-tissue interface, which is prone to electrochemical effects that can damage the probe and/or tissue. Recent work has demonstrated programmable micro-coil neural probes integrating CMOS technology with the micro-coil design. This work proposes a neural probe that co-optimizes a multi-turn micro-coil design with configurable CMOS current drivers for each micro-coil to maximize the induced electric field gradients. A four wire interface is used to multiplex power, deliver the stimulation current, and program the micro-coil current configuration. The proposed probes are characterized in a saline bath with a maximum stimulation current of 9 mA per 16-turn micro-coil, when simultaneously driving two micro-coils on a 3.5 V supply. Preliminary *in vitro* testing with mouse olfactory bulb slices and a commercial MEA show the probes are capable of producing changes in neural behavior.**

I. Introduction

Electrical stimulation delivered through implantable electrodes has allowed for the development of neural prostheses to restore sensory and motor functionality [1]. However, there are fundamental limitations with electrical stimulation using implantable electrodes that limit this approach. The produced electric fields are spatially symmetric, which prevent specific neurons from being targeted, limiting the effective stimulation spatial resolution [2]. Furthermore, glial scarring will increase the tissue impedance seen by the electrode and potentially prevent neurostimulation hardware from delivering the necessary current needed for eliciting neural behavior [3]. Finally, the electrode-tissue interface is prone to electrochemical effects that can damage the electrode and/or surrounding tissue if the charge transfer levels per phase are too high [4].

Magnetic stimulation through implantable micro-coils overcomes the addressed limitations of implantable electrodes. The induced electric fields from magnetic stimulation are spatially asymmetric and can avoid the activation of passing axons [5], [6]. Furthermore, magnetic fields have a high permeability to biological tissue and biocompatible materials. Therefore, the micro-coil-based stimulation efficacy is not weakened by glial scarring and can be completely encapsulated to eliminate the electrode-tissue interface. Recent developments in implantable micro-coil technology have produced devices capable of modulating neural behavior in *in vitro* and *in vivo* experiments. However, the lack of reconfigurable hardware in these devices fix their stimulation sites after implantation.

Recent work has utilized CMOS technology in the micro-coil design with additional nanofabrication processing to develop a neural probe capable of spatially programmable micro-coil magnetic stimulation [7]. However, that work did not use multi-turn micro-coil designs to decrease the necessary stimulation current. Furthermore, the design was one long programmable micro-coil that required very large switches in order to keep the micro-coil voltage below the transistor breakdown voltage during stimulation, reducing the current density, and thus, reducing the maximum induced electric field. The proposed neural probe co-optimizes the micro-coil design with integrated CMOS current drivers to provide spatially programmable neurostimulation sites from multi-turn, independently driven micro-coils. Furthermore, a four wire interface is implemented to use the current inputs and supply as the programming interface. This reduces the number of necessary terminals needed to connect the neural probe to external circuitry, reducing the packaging size.

II. Electromagnetic Simulations

For a device to stimulate neural tissue a sufficient gradient in the electric field must be produced along the axon of a neuron to generate local membrane depolarization. The electromagnetic derivation for the induced electric field gradients produced by the current flowing through a micro-coil can be found in [5]. Previous devices have shown that it is possible to induce sufficient electric field gradients by flowing current through a wire that travels down one edge of the probe, bends at the tip of the probe, and returns along the opposite edge [5], [6]. More recent work has shown that it is possible to utilize CMOS switching networks to change the location of the electric field gradients [7]. The proposed design improves upon this by eliminating the large switching networks and instead uses independently driven multi-turn micro-coils to change the location of the electric field gradients, while also reducing the stimulation current.

This work was supported by the NIH through the BRAIN Initiative (R01-NS110575), titled Investigating the Response of CNS Neurons to Electric and Magnetic Stimulation. This work was performed in part at the Cornell NanoScale Facility, an NNCI member supported by NSF Grant NNCI-2025233, and made use of the Cornell Center for Materials Research Shared Facilities, supported through the NSF MRSEC program (DMR-1719875).

[1] E. C. Szoka* and A. Molnar are with the Department of Electrical and Computer Engineering, Cornell University, Ithaca, NY 14853 USA (*corresponding author email: ecs227@cornell.edu).

[2] J. C. Werth and T. Cleland are with the Department of Psychology, Cornell University, Ithaca, NY 14853 USA

[3] S. Fried is with the Department of Neurosurgery, Massachusetts General Hospital (MGH), Harvard Medical School, Boston, MA 02114 USA and with the Boston VA Healthcare System, Boston, MA 02130 USA.

2021 IEEE Biomedical Circuits and Systems Conference (BioCAS) | 978-1-7281-7204-0/21/$31.00 ©2021 IEEE | DOI: 10.1109/BIOCAS49922.2021.9644971

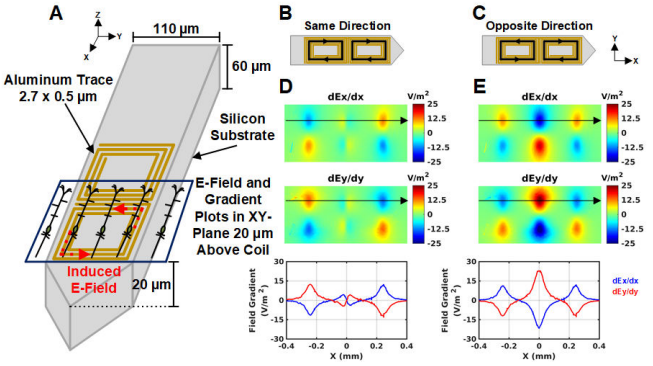

Fig. 1. Electromagnetic simulations for a neural probe with two multi-turn micro-coils under various current direction configurations. (A) Conceptual diagram for micro-coil based magnetic stimulation with the induced electric field direction shown for the bottom micro-coil current driven clockwise. (B) Neural probe with both micro-coils driven clockwise. Black lines show the current flow throughout the micro-coil used in the simulations. (C) Micro-coils driven in opposite directions. (D-E) Spatial gradients of the electric field along the x- and y-axes for the configurations used in B-C. Line plots show the field gradients along the x-axis over the upper stimulation sites.

Electromagnetic simulations are performed in COMSOL Multiphysics to predict the location and magnitudes of the induced electric field gradients produced by the micro-coils. The neural probe model is shown in Fig. 1 and consists of two closed loop micro-coils (consisting of four metal layers with four turns per metal layer) as well as a conductive silicon substrate etched in the shape of a probe. Micro-coil trace thickness and layer spacing are based on documentation provided by the foundry. The model is simulated under two states to compare the electric field gradients, and thus stimulation sites: micro-coil currents flowing in the same direction (clockwise) and opposite directions. The micro-coils and silicon probe are simulated in a rectangular prism of gray matter, similar to the models used in [6], [7].

Simulations are conducted with a 5 kHz sinusoid input stimulation current with an amplitude of 10 mA. Fig. 1D-E shows the x-axis and y-axis spatial gradients of the electric field for the two tested micro-coil current directions $20\,\mu\mathrm{m}$ above the probe, selected based on the size of the soma of typical neurons. When the currents are flowing in the same direction there are a pair of stimulation sites that appear above opposite corners of the micro-coils. The maximum gradients for dE/dx and dEy/dy are 12.24 and 12.34 V/m^2 respectively. There is also a smaller set of unintentional stimulation sites between the micro-coils where the maximum gradients for dE/dx and dEy/dy are 4.38 and 4.32 V/m^2 respectively. This is caused by the produced magnetic fields from the two micro-coils not completely cancelling out at their contiguous boundary.

When the micro-coil currents are flowing in opposite directions the strongest gradients appear between the two micro-coils. The maximum gradients for dE/dx and dE/dy are 21.72 and 22.89 V/m^2 respectively. The increased gradient strength is due to the current flow along the x-axis switching direction and the current flow along the y-axis doubling. The simulation results suggest that a neural probe can be designed with multiple multi-turn micro-coils where the desired stimulation sites are located between adjacent micro-coils, while reducing the total stimulation current from prior work by a factor of 7.5 [7]. The ability to predictably alter the location of the field gradients on the proposed probe suggests that different neuronal regions, such as individual layers of the neocortex, could be separately targeted.

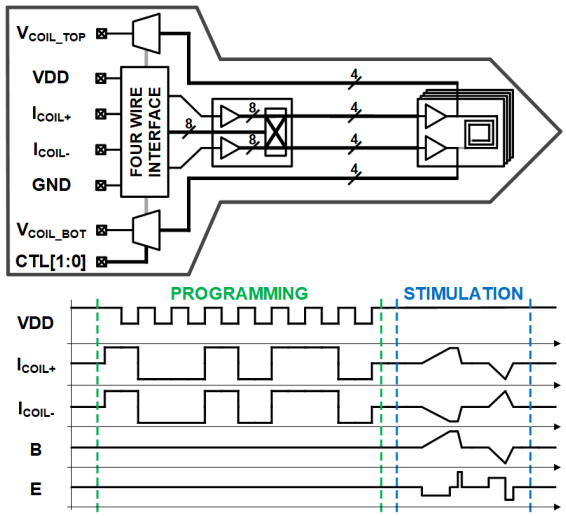

Fig. 2. System architecture of the proposed neural probe. Waveform plot shows an example of the supply, differential coil inputs, and expected magnetic and induced electric fields during programming and stimulation.

III. Neural Probe Design

A. System Overview

The proposed neural probe system is shown in Fig. 2. The backend circuitry of the probe contains a four wire interface to allow the supply and differential coil input terminals to double as the programming interface. The programming interface controls the state of the ternary (non-inverting, inverting, or off) push-pull current drivers to control which of a set of four separate micro-coils are active and the direction the current flows through them. This is implemented by passing both input current signals into a push-pull driver with eight parallel outputs, producing eight differential current pairs. Each output is cross-connected to its opposite-sign counterpart and routed down the probe to its dedicated micro-coil driver, with one such dedicated driver per micro-coil. When one driver output is active the cross-connected output is disabled. The micro-coils and their drivers are located near the tip of the probe, with the micro-coil terminals multiplexed off chip to characterize the maximum stimulation current.

Since it is not necessary to program the neural probe during stimulation, programming signals can be multiplexed with the power supply and differential stimulation current to use only four terminals. This decreases the number of necessary pads, thus decreasing the backend area and increasing the possible length of the insertable shank. During programming the supply cyclically drops beneath a threshold voltage, set by a PTAT driving a diode stack, to generate the programming clock. The common mode of the differential coil inputs serves as the programming data. This, in turn, moves the common mode of the micro-coils during programming; however, there is no current flowing through the micro-coils, and therefore there are no induced electric fields and no inadvertent stimulation during programming.

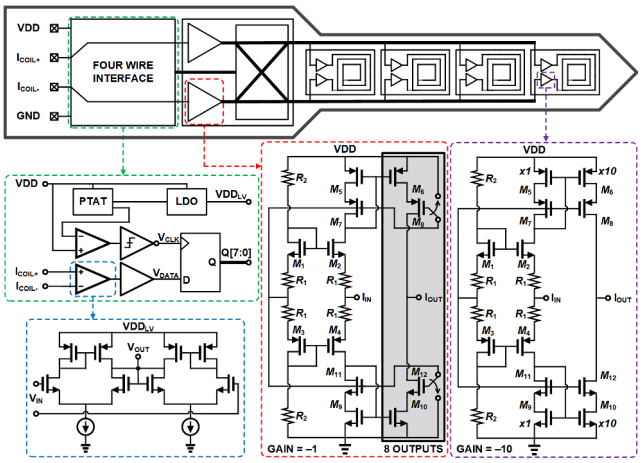

Fig. 3. Circuit implementation of the four wire interface, ternary current drivers, and micro-coil drivers.

B. Circuit Design

The circuit implementation of the four wire interface and push-pull current drivers is shown in Fig. 3. The supply of the four wire interface powers a PTAT to generate bias currents for amplifiers, current starved logic, and bias voltages. A low-dropout regulator produces a constant supply voltage for the digital circuitry. The clock is generated by comparing VDD to a bias voltage and is buffered by an inverting Schmitt trigger to prevent local drops in the digital supply voltage from generating multiple clock edges. The differential coil inputs are buffered by a pair of high output impedance differential pair amplifiers connected in unity gain feedback, with the common mode extracted by connecting the outputs of the amplifiers together. The programming bits are stored in a current starved shift register and are level shifted back to VDD to control the ternary push-pull drivers.

The ternary current drivers and micro-coil drivers use the same push-pull topology. Resistors R_1 trade-off between the input current range and the quiescent bias current. To further reduce the quiescent current transistor pairs M_1, M_2 and M_3, M_4 are introduced and operate in class AB mode. The output of the current driver is the parallel outputs of cascoded PFET and NFET current mirrors. Cascoded outputs are used to ensure accurate current mirroring over the wide range of coil voltages present during stimulation. The ternary driver outputs can be disabled by switching the PFET and NFET cascode gate voltages to supply and ground respectively. The output devices are sized such that the ternary current drivers have unity current gain and the micro-coil drivers have a current gain of ten.

C. Coil Optimization

The micro-coil design and push-pull amplifiers are co-designed to maximize the produced magnetic field. The maximum field is proportional to the total turns in the micro-coil and to the maximum current that can flow through the coil. Fig. 4 shows that the supply traces are routed long distances to the micro-coil drivers. Due to the parasitic resistance from the supply traces, it is advantageous to increase the number of turns per layer in the micro-coil, reducing the current for a given voltage across the coil, and lowering the voltage drop

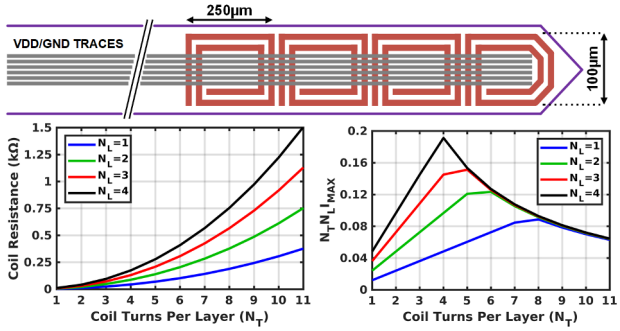

Fig. 4. Conceptual diagram showing long supply routing to coil drivers. Plots show the coil resistance and the maximum proportional magnetic field against the number of coil turns per layer for one through four metal layers.

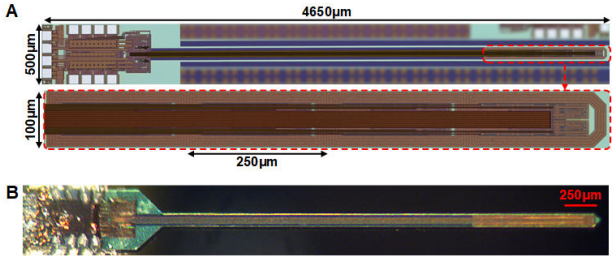

Fig. 5. Micrograph of the proposed probe. (A) Unreleased probe with zoom in on micro-coils with internal drivers. (B) Released and encapsulated probe.

across the supply traces. However, as the number of turns within an allotted coil area increases, the resistance scales super linearly because of increasing amounts of area spent on spacing between micro-coil turns.

Based on the resistivity of the traces and desired coil dimensions, an optimization shows the maximum magnetic field is produced when there is only one turn per layer (with four layers used). However, the required current to produce this maximum magnetic field cannot be achieved with reasonably sized current drivers. Therefore, an additional constraint to the coil optimization accounts for the maximum current that can be produced by a current driver that can fit inside the micro-coils. Fig. 4 shows the final optimization results with the maximum magnetic field produced using four metal layers with four turns per layer for a micro-coil with dimensions of 250 x 100 µm.

IV. Measurement Results

The neural probes were fabricated in a 180 nm 1P6M CMOS process and shown in Fig. 5. The probes are released using the nanofabrication process discussed in [7] and have a shank length and width of roughly 3900 µm and 110 µm respectively. Neural probes consist of four micro-coils using four metal layers to produce sixteen total turns with dimensions of 250 x 100 µm. The supply traces are routed as twenty alternating VDD/GND traces in the middle of the probe to ensure that the supply currents do not produce unintended magnetic fields. Three variations of the coils were fabricated where the current drivers are located either inside or outside the coil array and utilizing different metal layers for the micro-coil design.

Released micro-coils were characterized by sweeping the stimulation current and measuring the differential micro-coil voltages to determine the maximum stimulation current before coil driver saturation. Tests were done in room

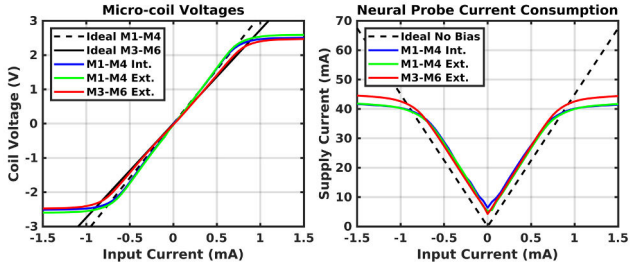

Fig. 6. Plots comparing the micro-coil voltage and supply current consumption against the neural probe input current.

temperature phosphate buffered saline and with stimulation waveforms similar to those used in [7]. Current-voltage plots are shown in Fig. 6 comparing the three micro-coil and driver configurations. The plots show that maximum stimulation current for the micro-coils using the bottom four metal layers is roughly 8.5 mA. The design using the top four metal layers shows a higher maximum stimulation current of 9 mA which is due to the thicker top metal layer, which reduces the resistance of the micro-coil and the headroom it consumes. Furthermore, since the top of the micro-coil is closer to the surface of the probe, the induced electric field gradients will be stronger than those from micro-coils using the bottom four metal layers. The current consumption plot shows the expected linear scaling of the current consumption until coil driver saturation, with variations in the bias currents across designs due to process variations affecting the bias points of the transistor pairs operating in class AB mode.

In vitro testing was done on 300 µm-thick mouse olfactory bulb slices with a commercial MEA. The tissue was horizontally sliced with a vibrating microtome and bathed with oxygenated aCSF at 34°C. Slices were aligned to the MEA by locating bands of spontaneous activity that indicate the mitral cell and external plexiform layers [8]. Spikes and LFPs were recorded using the 120-electrode MEA (MultiChannel Systems) with titanium nitride electrodes. The probe was placed on the surface of the slice with the micro-coils located over the region of tissue with visible activity. Testing consisted of driving the micro-coils with stimulation trains of fifty 10 Hz ramp waveforms (1 mA peak amplitude input current, 50% duty cycled, negative ramp polarity) spaced ten seconds apart while observing changes in neural behavior.

Recorded data are zero-phase (forward and reverse) re-filtered between 300 Hz - 3 kHz prior to offline spike sorting and unit identification using WaveClus [9]. Unit identification is able to differentiate between spikes and stimulation artifacts of similar amplitudes. Fig. 7 shows preliminary results using a neural probe with micro-coils using the bottom four metal layers and internal drivers. The micro-coil is configured to have the two inner coils run current in opposite directions to generate the strongest gradient in the electric field, while the outer coils are disabled. The dot plot shows that the stimulation waveform has an inhibitory effect on the recorded activity, consistent with the results found in [7], while reducing the stimulation power consumption by a factor of five. On-going tests are studying the statistical significance of the inhibitory effect, the spatial extent of the neural response, and performance of various probe designs.

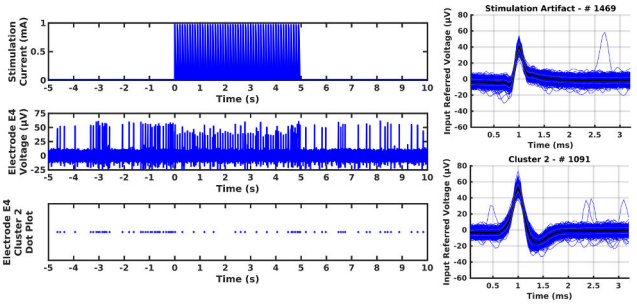

Fig. 7. Preliminary data showing inhibitory neural response to stimulation train and the time-aligned spikes and stimulation artifacts identified by [9].

V. Conclusion

This work proposes a neural probe that co-optimizes the micro-coil design with CMOS current drivers to maximize the electric field gradients and reduce the necessary stimulation current. Independently driven multi-turn micro-coils allow for spatially programmable neurostimulation sites between adjacent micro-coils. A four wire interface is used to reduce the number of pads on the probe backend by using the supply and differential current inputs as the programming clock and data signals respectively. The electrical performance of the probes is characterized in a phosphate buffered saline bath. Preliminary *in vitro* testing of the neural probes is done with slices of a mouse olfactory bulb in conjunction with an MEA showing changes in neural behavior.

Acknowledgement

The authors would like to thank Seung Woo Lee for technical discussions on micro-coil magnetic stimulation, Sunwoo Lee for discussions on nanofabrication processing, and Matthew Einhorn for assistance with the MEA hardware.

References

[1] S. J. Bensmaia and L. E. Miller, "Restoring sensorimotor function through intracortical interfaces: progress and looming challenges," *Nature Reviews Neuroscience*, vol. 15, no. 5, pp. 313–325, 2014.

[2] M. R. Behrend, A. K. Ahuja, M. S. Humayun, R. H. Chow, and J. D. Weiland, "Resolution of the epiretinal prosthesis is not limited by electrode size," *IEEE Transactions on Neural Systems and Rehabilitation Engineering*, vol. 19, no. 4, pp. 436–442, 2011.

[3] W. M. Grill, S. E. Norman, and R. V. Bellamkonda, "Implanted neural interfaces: Biochallenges and engineered solutions," *Annual Review of Biomedical Engineering*, vol. 11, no. 1, pp. 1–24, 2009.

[4] S. F. Cogan, K. A. Ludwig, C. G. Welle, and P. Takmakov, "Tissue damage thresholds during therapeutic electrical stimulation," *Journal of Neural Engineering*, vol. 13, no. 2, p. 021001, jan 2016.

[5] S. W. Lee, F. Fallegger, B. D. F. Casse, and S. I. Fried, "Implantable microcoils for intracortical magnetic stimulation," *Science Advances*, vol. 2, no. 12, 2016.

[6] S. W. Lee, K. Thyagarajan, and S. I. Fried, "Micro-coil design influences the spatial extent of responses to intracortical magnetic stimulation," *IEEE Transactions on Biomedical Engineering*, vol. 66, no. 6, pp. 1680–1694, June 2019.

[7] E. C. Szoka, J. C. Werth, S. Lee, J.-I. Lee, A. J. Cortese, T. A. Cleland, S. Fried, and A. Molnar, "Neural probe utilizing programmable micro-coil magnetic stimulation," in *2021 10th International IEEE/EMBS Conference on Neural Engineering (NER)*, 2021, pp. 651–654.

[8] S. T. Peace, B. C. Johnson, G. Li, M. E. Kaiser, I. Fukunaga, A. T. Schaefer, A. C. Molnar, and T. A. Cleland, "Coherent olfactory bulb gamma oscillations arise from coupling independent columnar oscillators," *bioRxiv*, 2017.

[9] F. J. Chaure, H. G. Rey, and R. Quian Quiroga, "A novel and fully automatic spike sorting implementation with variable number of features," *Journal of Neurophysiology*, vol. 120, no. 4, pp. 1859–1871, 2018.